



Alignment correction for plane grating monochromator using the c_{ff} parameter

Alisa Danilenko

*School of Physics and Astronomy, University of St Andrews, Scotland
DESY, Hamburg, Germany*

September 6, 2017

Abstract

This report describes the search for a new, faster method to correct alignment errors in the monochromator section of Beamline P04 at the PETRA III synchrotron, located at DESY, Hamburg. The method is based on the premise of changing the monochromator's fix focus constant. If there is a misalignment in the beamline, spectra taken at differing c_{ff} values show significant shifts in energy. By introducing deliberate misalignments and analysing their effect, one can detect the offset in the system and correct for it. This allows for faster and more methodical calibration of the beamline.

Supervisor: Dr. Jens Buck

Contents

1	Introduction	3
1.1	Beamline layout	3
1.2	Motivation	3
1.3	XRT simulation	3
1.4	Argus Spectrometer	4
2	Methods	4
2.1	Simulation	4
2.1.1	Solving for α and β	5
2.1.2	Solving for mirror and grating angles	5
2.1.3	Translational corrections	5
2.1.4	Output	7
2.1.5	Data collection	7
2.2	Au XPS with Argus	8
3	Results	9
3.1	Mirror offset	9
3.2	Grating offset	10
4	Conclusions	10

1 Introduction

1.1 Beamline layout

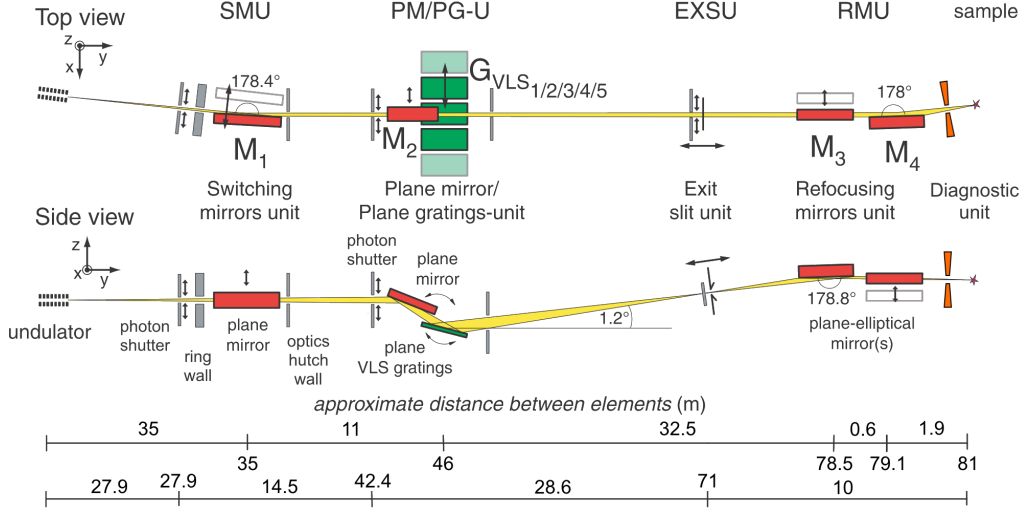


Figure 1: Full layout, PETRA III Beamline P04¹

The monochromator section of Beamline P04 consists of a plane pre-mirror, a VLS (variable line spacing) grating, and an exit slit. The exit energy is selected by moving the grating, and adjusting the pre-mirror accordingly. The fix focus constant is defined in Equation 1, where α and β are the entrance and exit angles of the beam onto the grating, respectively.

$$c_{ff} = \frac{\cos(\beta)}{\cos(\alpha)} \quad (1)$$

1.2 Motivation

Proper alignment is a crucial part of beamline commissioning procedure. Optical component positions can sometimes drift, or be set inaccurately by the software control motors, which may overshoot or not quite reach the calculated positions. Due to the precise nature of the machinery and the experiments conducted on it, a small error in monochromator component alignment can cause a significant shift in the exit energy, which needs to be corrected or accounted for in experiments.

c_{ff} can be implemented in this alignment correction, because theoretically, at perfect alignment, a change in c_{ff} should not bring about a shift in the exit energy of the monochromator. Measuring at different c_{ff} values, one can observe a shift in energy, determining that there is indeed a misalignment. By deliberately introducing errors into the angles of the optical components, we attempt to track the effects of these misalignments and correct for them as much as possible using an iterative method.

The investigation was effectively split into two parts: the first involved simulating the monochromator setup using xrtQook, a ray tracing software package. The second was obtaining experimental results using the Argus spectrometer at beamline P04. The results from the simulation and the experiment were then compared.

1.3 XRT simulation

XRayTracer (xrt) is a Python software library which can be used for ray tracing in the x-ray regime³. The library also gives the user the option of using wave propagation, but in this project only the ray tracing features were required. A GUI tool for creating scripts, xrtQook, is included. This is used in this investigation to model the monochromator section of the beamline.

1.4 Argus Spectrometer

Experimental results in this investigation were taken using the dynamic-XPS end station for beamline P04². The station consists of three chambers. These are kept under UHV conditions by turbomolecular pumps, and are separated by gate valves. Samples are introduced into the load lock and transferred into the preparation chamber using a magnetically coupled transfer. Equipped with a quartz microbalance and a sputtering gun, this chamber is used for sample processing. This was not necessary for the investigation described, as we used a simple Au sample. The samples are then transferred to the analysis chamber. There, they can be moved by the manipulator with 4 degrees of freedom; x, y, z, and azimuthally about the z axis. The position for measurements is located near the center of the chamber.

Electrons ejected from the sample are collected by the Argus spectrometer. The user controls the lens voltages and therefore the pass energy, as well as the aperture size. For XPS measurements, the spectrometer is usually operated in Constant Analyser Energy (CAE) mode, in which pass energy E_p is kept constant across a scan of selected kinetic energies.

2 Methods

2.1 Simulation

xrtQook was used to model the monochromator section of the beamline. The model contains an undulator as the source, and the global coordinate system is defined as $[0,0,0]$ at the source. The beam points along the y axis. The settings of the undulator are defined in accordance with those used in the undulator at P04, and it is set to propagate 5 million rays through the setup per run. The output energy is also set by the user. For this investigation, 1000 ± 50 eV. The optical components in the model include a plane mirror, coated with Platinum, tilted at angle a with respect to the y axis, and a plane grating tilted at angle b . The grating used for this dataset is set to a groove density of 1200/mm. One of the differences between the simulation and reality must be highlighted here; while the grating used in the simulation is a plane grating with regular line spacing, the grating implemented in the physical monochromator at beamline P04 is actually a VLS (variable line spacing) grating, which is not yet available in xrt.

The aperture, width 1mm, is positioned at a fixed distance z_2 above the undulator axis. The basic setup is shown in Figure 2.

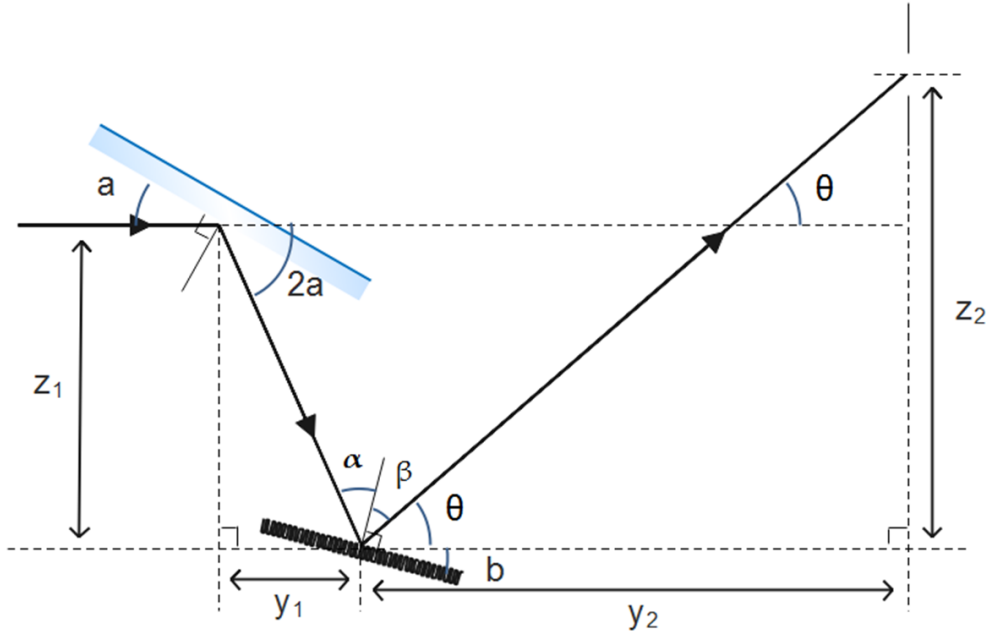


Figure 2: The basic setup

2.1.1 Solving for α and β

$$c_{ff} = \frac{\cos(\beta)}{\cos(\alpha)} \quad (1)$$

$$\sin(\alpha) + \sin(\beta) = Nk\lambda \quad (2)$$

In order to set a specific c_{ff} value, values of α and β that satisfy both the c_{ff} equation (1), and the Grating Equation (2) for a reflective grating must be found. (1) and (2) are solved simultaneously, obtaining

$$\beta = \arcsin\left(\frac{c_{ff}^2 Nk\lambda - \sqrt{1 + c_{ff}^4 + c_{ff}^2((Nk\lambda)^2 - 2)}}{c_{ff}^2 - 1}\right) \quad (3)$$

$$\alpha = \arcsin\left(\frac{-Nk\lambda + \sqrt{1 + c_{ff}^4 + c_{ff}^2((Nk\lambda)^2 - 2)}}{c_{ff}^2 - 1}\right) \quad (4)$$

Following the convention that β is negative.

2.1.2 Solving for mirror and grating angles

We now need to find the angles at which the pre-mirror and grating should be pitched so as to achieve a certain c_{ff} while maintaining a constant θ , so that the desired harmonic of the beam always hits the fixed exit slit. These angles are labeled a and b respectively. We see that

$$2a + \alpha - \beta + \theta = 180 \quad (5)$$

$$b + \theta - \beta = 90 \quad (6)$$

Combining these, we find

$$b = 90 + \arcsin\left(\frac{c_{ff}^2 Nk\lambda - \sqrt{1 + c_{ff}^4 + c_{ff}^2((Nk\lambda)^2 - 2)}}{c_{ff}^2 - 1}\right) - \theta \quad (7)$$

$$a = \frac{1}{2}(90 + b - \alpha) = \frac{1}{2}(180 + \arcsin\left(\frac{c_{ff}^2 Nk\lambda - \sqrt{1 + c_{ff}^4 + c_{ff}^2((Nk\lambda)^2 - 2)}}{c_{ff}^2 - 1}\right) - \theta - \arcsin\left(\frac{-Nk\lambda + \sqrt{1 + c_{ff}^4 + c_{ff}^2((Nk\lambda)^2 - 2)}}{c_{ff}^2 - 1}\right)) \quad (8)$$

2.1.3 Translational corrections

It must be ensured that the beam from the pre-mirror hits the center of the grating at any set c_{ff} . Here, two methods of achieving this are outlined; the first involves y and z translation of the grating, while the second is simply a y correction to the pre-mirror position.

Method 1: grating translation

We choose a 'reference setup' in which we know that the beam from the pre-mirror hits the centre of the grating. Here a vertical separation of 15mm and a horizontal one of 200mm is used. The positioning of the grating is then adjusted based on the changes in the pre-mirror angle a .

$$\tan(\theta) = \frac{\delta z}{\delta y} \quad (9)$$

$$\tan(90 - 2a) = \frac{200 + \delta y}{15 - \delta z} \quad (10)$$

Solving simultaneously, we find

$$\delta y = \frac{5(3 \tan(90 - 2a) - 40)}{1 + \tan(90 - 2a) \tan(\theta)} \quad (11)$$

$$\delta y = \frac{5 \tan(\theta)(3 \tan(90 - 2a) - 40)}{1 + \tan(90 - 2a) \tan(\theta)} \quad (12)$$

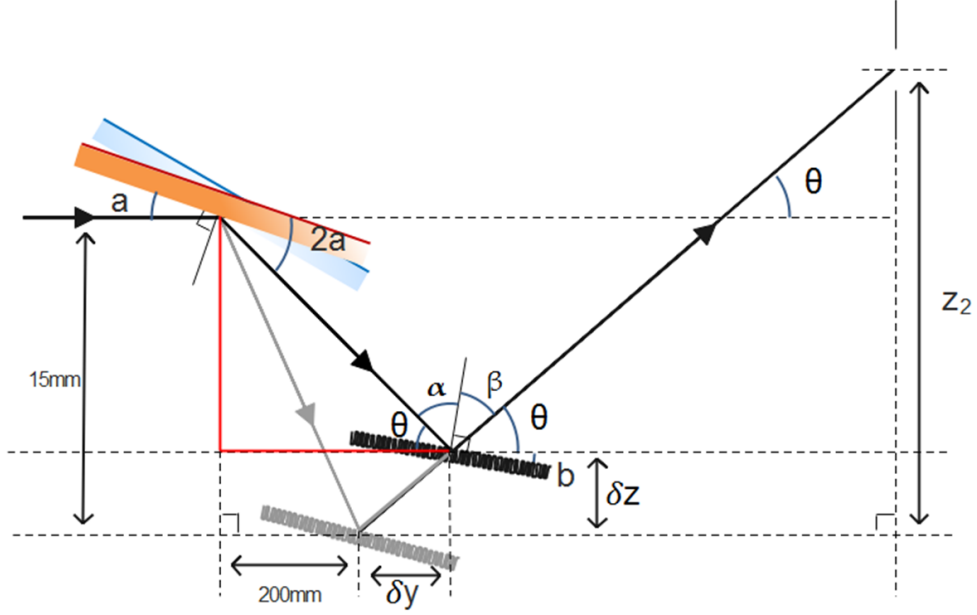


Figure 3: grating translation

Method 2: mirror translation

Again, we start with the same 'reference setup'. This time, the mirror position is adjusted. The vertical distance between mirror and grating centers remains unchanged. This second method is implemented in the simulation for this investigation.

$$\tan(90 - 2a) = \frac{200 + \delta y}{15} \Rightarrow \delta y = 15 \tan(90 - 2a) - 200 \quad (13)$$

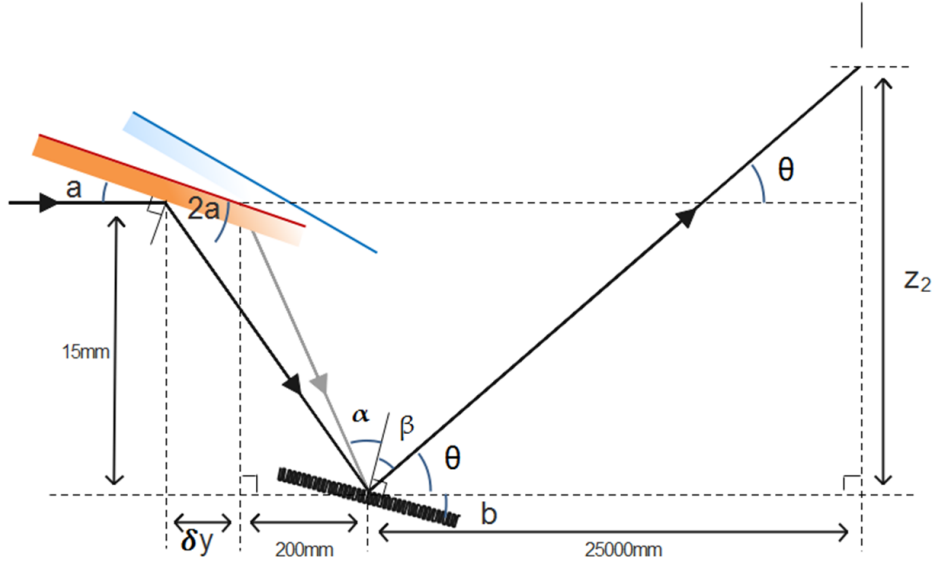


Figure 4: mirror translation

2.1.4 Output

Screens are inserted into the setup to view and analyse the beam at a chosen point. In this case, screens were placed directly in front of and behind the aperture, so that both the effect of the grating and the beam exiting the aperture can be observed. An example of the code output is shown in Figure 5.

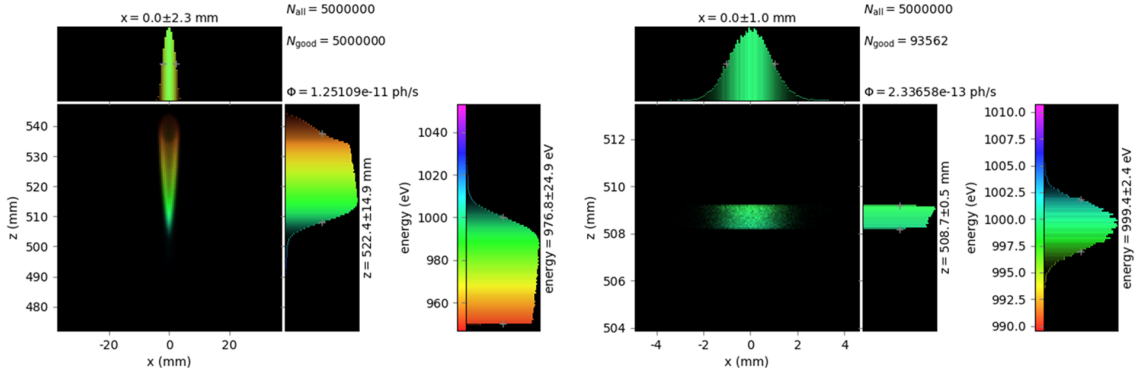


Figure 5: xrt output, $c_{ff} = 2$

xrt outputs a cross sectional view of the beam at the chosen position, with histograms in y and z, as well as an energy histogram. Using this energy histogram, one can track energy shifts in the output spectra.

2.1.5 Data collection

In order to collect data that could be compared with experimental results, errors were introduced to a , the calculated angle of the pre-mirror. This was done in the range ± 0.00008 radians, in steps of 0.00001 radians. Graphs were plotted of the shift in energy with respect to the spectrum at $c_{ff} 2$ with no introduced defects against the mirror angle defect for different values of c_{ff} , with the hope of finding a point of intersection between the plots for different c_{ff} values, indicating the necessary correction to the mirror angle. This is the data later used to compare with the physical experiment.

Another set of data was collected to observe the effect of grating motion on the output energy. For this, the aforementioned scans were repeated, with a lower resolution, for a range of grating angle defects.

2.2 Au XPS with Argus

Measurements were performed using the dynamic XPS end station in CAE mode, using medium magnification, a pass energy of 20 eV and a 20 micron exit slit.

Alignment was performed focusing on the $4f_{7/2}$ and $4f_{5/2}$ peaks in the Au spectrum, defined as having electron binding energies of 87.6 eV and 84.0 eV respectively⁵. A reference scan was taken in the kinetic energy range of 885 eV to 945 eV, in small steps of 0.02 eV. All further measurements were then taken within the region of interest of 905 eV to 925 eV. Due to the large exit slit size and pass energy, dwell time was able to be reduced to just 0.1 seconds.

Data was acquired by introducing errors to the position of the pre-mirror in the monochromator using the software controlled motors, and obtaining spectra at each step. This was performed in the range ± 0.0032 degrees, in steps of 0.0008 degrees. Each measurement was repeated three times. This was done for c_{ff} values of 2.011 (the standard setting used for usually at the beamline), 1.5, and 4.

Using a matlab script⁴ the relative peak shift of the new spectrum was determined for each measurement as the center of gravity of the so-called 'shift spectrum', built up from the non-negative coefficients for shifted copies of the reference spectrum whose superposition best reproduces the new spectrum. This optimisation was determined in terms of a least squares fit.

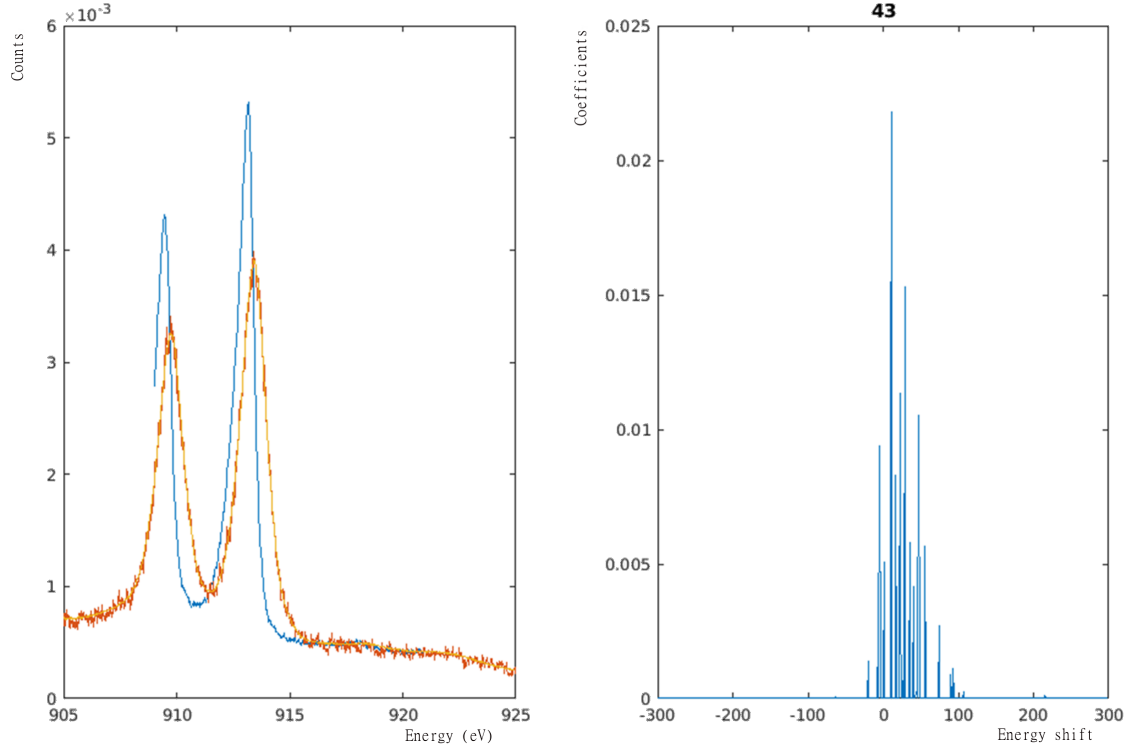


Figure 6: This is an example of the procedure used to find energy shifts in the measured spectra. On the left, the spectrum measured at c_{ff} 4 with a mirror defect of $80 \mu\text{radians}$ is shown in red, along with the reference spectrum in blue. The yellow line shows the superimposed copies of the reference spectrum multiplied by the shift spectrum coefficients, in an attempt to reproduce the new spectrum. The shift spectrum itself, whose center of gravity indicates the energy shift of the measured spectrum with respect to the reference, is shown on the right.

The energy shift was then plotted against the pre-mirror angle offset for each of the three c_{ff} values, with the angular offsets converted to radians to match the units used in the simulation.

3 Results

3.1 Mirror offset

It is important to note here that there may be an unknown bug in the xtr code or the software itself, as according to the calculations in section 2.1 the exit energy should be the same at every c_{ff} value providing the setup is in the correct configuration. In the fitted simulation results, however, we see that there is no one point where the exit energy is exactly the same for every c_{ff} value, but there is a point of closest approach. We focus on the analysis of c_{ff} values 1.5, 2, and 4, as these are the ones that were observed experimentally. The simulation data for these is shown in Figure 7. The three lines, representing the three c_{ff} values, form a small triangle rather than crossing at one point.

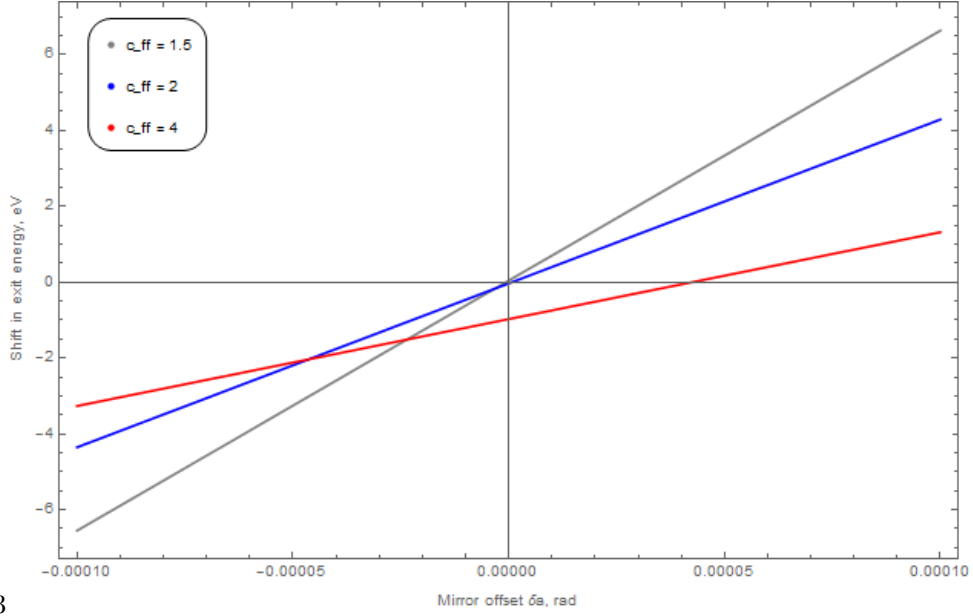


Figure 7: Mirror offset effect on energy shift, simulation

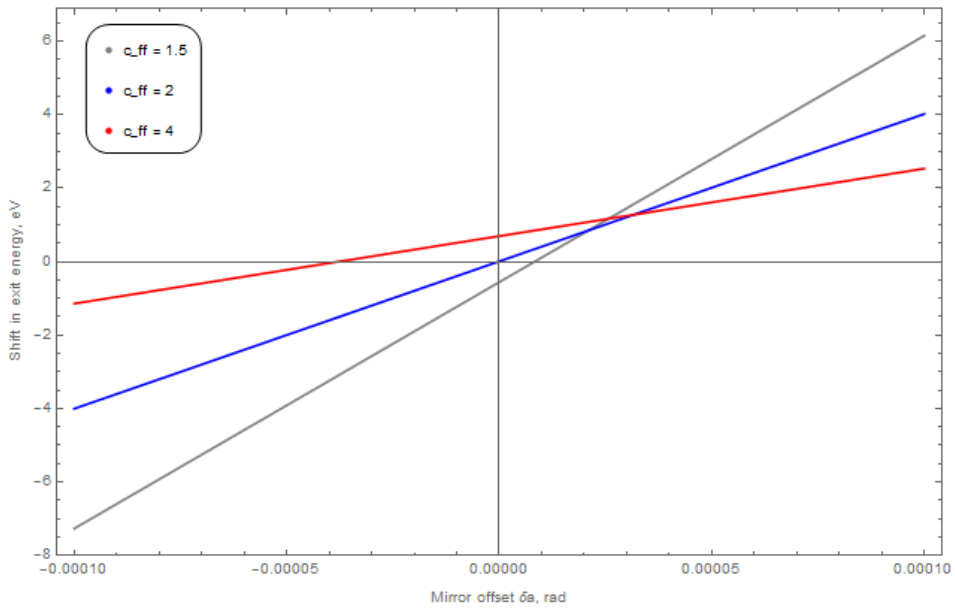


Figure 8: Mirror offset effect on energy shift, experiment

In the experimental data we see a similar result to the simulation, in that the lines do not cross exactly at one point, but do have a point of closest approach. The 'ideal' intersection points occur at different offset angles in the simulation and experiment; experimental results show the optimal mirror offset to be $26 \mu\text{radians}$, while the simulation shows the point of closest approach at $-24 \mu\text{radians}$. The energy shifts at these values are also different, with 1.14 eV in the experimental data and -1.320 eV in simulation. Here again we see the effect of the unknown bug, as the idealised simulation should have an exact crossing point at $\delta a = 0$, and at the exact set energy. One possible explanation for the offset is the method used to determine the experimental shifts in energy: while effective, it does not take background noise into account, and some seemingly artificial artifacts have been observed in the 'shift spectra', meaning that the shifts calculated may be subject to some offset we are not aware of.

However, there is a qualitative match between what we see in the simulation and the experimental result: in both, there is an optimised mirror angle in which the energy shifts for various c_{ff} values are very similar. The experimental and simulated gradients of the lines for each c_{ff} value are within 20% of each other. This tells us that it is worth pursuing an alignment method based on c_{ff} .

3.2 Grating offset

Offsetting the pitch of the grating causes a perfectly linear change in exit energy. The smaller the angle b , the higher the exit energy. As mentioned before, scans through different mirror pitch offsets at c_{ff} values 1.5, 2, and 4 were performed, and the results compared. The 'triangle' formed at the intersection of the linear fits for the three c_{ff} values was observed to move with changes in grating angle; this is demonstrated in Figure 9, which tracks the position of the bottom corner of the triangle. In the observed region, the data fits well to a third order polynomial.

Since it can be seen that motion of the grating causes a movement of the intersection region, it is possible that some discrepancy between simulation and reality is explained by the position of the grating, which was not changed during experimental measurement, but may have been slightly offset the entire time.

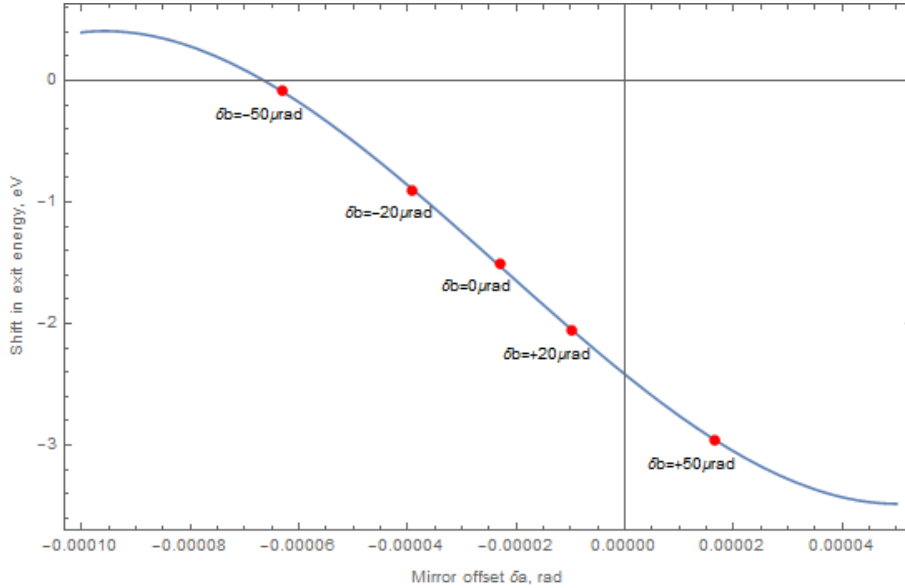


Figure 9: Tracking the motion of the intersection region with changing grating angle b .

4 Conclusions

While the simulation and the experiment do not match directly, they show that there is a way of finding the mirror angle correction for optimal alignment using the c_{ff} parameter. With the tendency of optical components to drift and the inability of the motors to make totally exact angle changes, the proposed method of optimising alignment would have to be iterative.

The exact development of the method could be facilitated in future work if a more accurate simulation of the experiment could be produced, without unexplained shifts in the simulated spectra. A VLS grating add on for the xrt software is already in the works, which will improve the accuracy of the simulation.

The idea would be to take two measurements, at different mirror offsets, at each of two different c_{ff} values, and fit two lines. Then, the intersection point of these two lines would be taken as the new 'zero offset' point, and the process would be repeated until the beam is satisfactory. This proposed process would require four data points per iteration; at the current settings this means eight minutes per iteration, which is very reasonable.

The findings regarding grating motion could be utilised also; moving the mirror allows the user to align the components such that there is an optimal point at which all c_{ff} values give a nearly identical result, but there is a possibility that grating movement would allow for the translation of this point to the desired energy shift, ie. the shift could be eliminated altogether.

References

1. http://photon-science.desy.de/facilities/petra_iii/beamlines/p04_xuv_beamline/beamline_layout/index_eng.html
2. Investigation of advanced materials based on low-dimensional systems, S. Babenkov, Hamburg, 2016
3. Authors K. Klementiev, MAX IV Lab, R. Chernikov, Canadian Light Source, 2017
<http://pythonhosted.org/xrt/>
4. J. Buck, DESY, 2016
5. X-RAY DATA BOOKLET, A. Thompson et al, Center for X-ray Optics and Advanced Light Source, Lawrence Berkley National Laboratory, 2011